

Many-body Theory vs Simulations for the pseudogap in the Hubbard model

S. M. Oukouri, S. A. Ille, F. Lévy, B. K. Yang, D. Poulin, Y. M. Vilk¹ and A. M. S. Tremblay²

Département de physique and Centre de recherche en physique du solide

²Institut canadien de recherches avancées

Université de Sherbrooke, Sherbrooke, Québec, Canada J1K 2R1.

¹2100 Valencia Dr. apt. 406, Northbrook, IL 60062

(March 3, 2019)

The opening of a critical fluctuation induced pseudogap in the one-particle spectral weight of the half-filled two-dimensional Hubbard model is discussed. This pseudogap, appearing in our Monte Carlo simulations, may be obtained from many-body techniques that use Green functions and vertex corrections that are at the same level of approximation. Self-consistent theories of the Eliashberg type (such as the Fluctuation Exchange Approximation) use renormalized Green functions and bare vertices in a context where there is no Migdal theorem. They do not find the pseudogap, in quantitative and qualitative disagreement with simulations, suggesting these methods are inadequate for this problem.

The two-dimensional Hubbard model is one of the key paradigms of many-body Physics and is extensively studied in the context of the cuprate superconductors. While there is now a large consensus about the fact that at half-filling ($n = 1$) the ground state is antiferromagnetic, [1,2] the route to this low-temperature phase is still a matter of controversy. While we know that the Fermi-Wagner theorem precludes an antiferromagnetic phase transition at finite temperature, the issue of whether there is, or not, a precursor pseudogap at finite temperature in the single-particle spectral weight $A(k_F; \omega)$ is still unresolved, despite the fact that the answer to this question is important to understand the normal state of high-temperature superconductors. Different many-body approaches give qualitatively different answers to this pseudogap question. In particular, the widely used self-consistent Fluctuation Exchange Approximation (FLEX) [3] does not find a pseudogap in the $d = 2$ repulsive Hubbard model for any filling. A study [4] of lattices of up to $L = 128$ found that as the temperature is reduced the quasiparticle peak in $A(k_F; \omega)$ smear considerably while remaining maximum at $\omega = 0$, signaling a deviation from the Fermi liquid behavior but no pseudogap. The same qualitative answer is found for attractive models. By contrast, the many-body approach that has given to date the best agreement with simulations of both static [5] and imaginary-time quantities [6] concludes to the existence of a pseudogap in the weak to intermediate coupling regime.

One may think that numerical results have already resolved the pseudogap issue but this is not so. Early Quantum Monte Carlo (QMC) data analytically contin-

ued by the Maximum Entropy method concluded that precursors of antiferromagnetism in $A(k_F; \omega)$ were absent at any non-zero temperature in the weak to intermediate coupling regime ($U < 8t$, U is the Coulomb repulsion term and t the hopping parameter) [8]. A subsequent study in which a singular value decomposition technique was used instead of Maximum Entropy, concluded to the opening of a pseudogap in $A(k_F; \omega)$ at low temperatures [9]. Each of the two techniques has limitations. The singular value decomposition can achieve a better resolution at low frequencies, but we find that the quality of the spectra is influenced by the profile function introduced to limit the range of frequencies. Another difficulty is that it leads to negative values of $A(k_F; \omega)$. As far as Maximum Entropy is concerned, recent advances [10], that we will use here, have made this method more reliable than the classic version applied in Ref. [8].

In this paper, we address the issue of the pseudogap in the $d = 2; n = 1$ Hubbard model at weak to intermediate coupling, but it will be clear that the general conclusions are more widely applicable. We present QMC results and show that the finite-size behavior obtained for $A(k_F; \omega)$ is correctly reproduced by the method of Ref. [7]. We also introduce a slight modification of the latter approach that makes the agreement even more quantitative. This many-body approach allows us to extrapolate to infinite size and show that the pseudogap persists even in lattices whose sizes are greater than the antiferromagnetic correlation length, contrary to the statements made earlier [8]. These sizes cannot be reached by QMC when the temperature is too low. We confirm that at low enough temperatures, the peak at $\omega = 0$ at the Fermi wave vector is replaced by a minimum, corresponding to the opening of a pseudogap [7] and by two side peaks that are precursors of the Bogoliubov quasiparticles. In contrast, we find that the $A(k_F; \omega)$ calculated by FLEX on small lattices are qualitatively different from those of QMC and do not have the correct size dependence. Since all many-body techniques involve some type of approximation, their reliability should be gauged by their capacity to reproduce, at least qualitatively, the Monte Carlo results in regimes where the latter are free from ambiguities. We thus conclude that Eliashberg-type approaches such as FLEX are unreliable in the absence of a Migdal theorem and that there is indeed a pseudogap in the weak to intermediate coupling regime at half-filling. Consistency between the Green functions and vertices used in the many-body

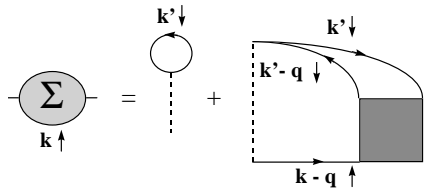


FIG. 1. Formally exact diagrammatic representation of the self-energy in the Hubbard model. The square is the fully reducible four-point vertex

calculation seems crucial to obtain the pseudogap.

Many-body techniques of the paramagnon type [11] do lead to a pseudogap but they usually have low-temperature problems because they do not satisfy the Mermin-Wagner theorem. No such difficulty arises in the approach of Ref. [7]. In this method there are only two momentum- and frequency-independent irreducible particle-hole vertices. The spin and charge susceptibilities $_{sp}^1(q) = _0(q)^1 - \frac{U_{sp}}{2}$ and $_{ch}^1(q) = _0(q)^1 + \frac{U_{ch}}{2}$ satisfy conservation laws, the Mermin-Wagner theorem, as well as the Pauli principle $n^2 = hn$ implicit in the following two sum rules

$$\frac{T}{N} \sum_q X_{sp}(q) = \frac{D}{(n - n_{\#})^2} = n + 2hn \cdot n_{\#} \quad (1)$$

$$\frac{T}{N} \sum_q X_{ch}(q) = \frac{D}{(n + n_{\#})^2} = n^2 = n + 2hn \cdot n_{\#}$$

where n is the density. We use the notation, $q = (q; iq_n)$ and $k = (k; ik_n)$ with iq_n and ik_n respectively bosonic and fermionic Matsubara frequencies. We work in units where $k_B = 1$; $h = 1$; lattice spacing and hopping t are unity. The above equations, in addition to [5] $U_{sp} = U hn \cdot n_{\#} = (hn \cdot hn_{\#})$, suffice to determine the constant vertices U_{sp} and U_{ch} . This Two-Particle Self-Consistent approach will be used throughout this paper, unless we refer to FLEX calculations. The single-particle self-energy is calculated after the spin and charge susceptibilities. In the original approach [6] it reads

$$^{(1)}(k) = U n + \frac{U T}{4 N} \sum_q [U_{sp} X_{sp}(q) + U_{ch} X_{ch}(q)] G^0(k + q) \quad (2)$$

The vertices U_{sp} and U_{ch} as well as $G^0(k + q)$ are the same quantities that enter the susceptibilities above.

There is, however, an ambiguity in the self-energy formula. Within the assumption that only U_{sp} and U_{ch} enter as irreducible particle-hole vertices, the self-energy expression in the transverse spin fluctuation channel is

different. To resolve this paradox, consider the exact formula for the self-energy represented symbolically by the diagram of Fig. 1. In this figure, the square is the fully reducible vertex $(q; k - k^0; k + k^0 - q)$: In all the above formulas, the dependence of q on $k + k^0 - q$ is neglected since the particle-particle channel is not singular. The longitudinal version of the self-energy Eq. (2) takes good care of the singularity of q when its first argument q is near $(0, 0)$: The transverse version does the same for the dependence on the second argument $k - k^0$, which corresponds to the other particle-hole channel. One then expects that averaging the two possibilities gives a better approximation for q since it preserves crossing symmetry in the two particle-hole channels. Furthermore, one can verify that the longitudinal spin fluctuations in Eq. (2) contribute an amount $U hn \cdot n_{\#} i = 2$ to the consistency condition [6] $\frac{1}{2} \text{Tr}^{(1)} G^0 = U hn \cdot n_{\#} i$ and that each of the two transverse spin components also contribute $U hn \cdot n_{\#} i = 2$ to $\frac{1}{2} \text{Tr}^{(2)} G^0 = U hn \cdot n_{\#} i$: Hence, averaging Eq. (2) and the expression in the transverse channel also preserves rotational invariance. In addition, one verifies numerically that the exact sum rule [7]

$d!^0 \text{Im}[(k; !^0)] = U^2 n (1 - n)$ determining the high-frequency behavior is satisfied to a higher degree of accuracy. We will thus use a self-energy formula that we call "symmetric"

$$^{(s)}(k) = U n + \frac{U T}{8 N} \sum_q [3U_{sp} X_{sp}(q) + U_{ch} X_{ch}(q)] G^0(k + q) \quad (3)$$

$^{(s)}(k)$ is different from so-called Berk-Schrieffer type expressions [11] that do not satisfy [7] the consistency condition between one- and two-particle properties, $\frac{1}{2} \text{Tr} G^0 = U hn \cdot n_{\#} i$:

In comparing the above self-energy formulas with FLEX, it is important to note that the same renormalized vertices and Green function appear in both the conserving susceptibilities and in the self-energy formula Eq. (3). In the latter, one of the external vertices is the bare U while the other is dressed (U_{sp} or U_{ch} depending on the type of fluctuation exchanged). This means that the fact that Migdal's theorem does not apply here is taken into account. This technique is to be contrasted with the FLEX approximation where all the vertices are bare ones, as if there was a Migdal theorem, while the dressed Green functions appear in the calculation. In this Eliashberg-type self-consistent approach then, the Green functions are treated at a high level of approximation while all the vertices are bare, zeroth order ones. In other words, the basic elements of the perturbation theory are treated at extremely different levels of approximation.

Our Monte Carlo results were obtained with the determinant method [2] using typically 10^5 Monte Carlo updates per space-time point. The inverse temperature is $\beta = 5$, the interaction strength is $U = 4$ and periodic boundary conditions on a square lattice are used.

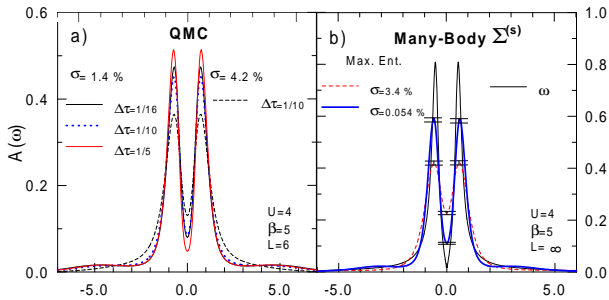


FIG. 2. For $U = 4$, $\beta = 5$, $n = 1$, $k = (0; \cdot)$, effect of various other calculational parameters: (a) QMC for $L = 6$. Thick dotted line for $\Delta t = 1/10$ and $\sigma = 1.4\%$. The latter is the average of the error on $G(\cdot)$ normalized by $G(\cdot)$ itself. Calculations with the same Δt but for $\Delta t = 1/5$ and $1/16$ are also shown. Thin dashed line is for $\Delta t = 1/10$ but $\sigma = 4.2\%$ on $G(\cdot)$. (b) Thin solid line, real-frequency calculation using Eq.(3), for an infinite system. Also shown, Maximum Entropy inversion of $G(\cdot)$ with same Δt as in Fig.3 and a smaller one.

Other details about the simulation may be found in the captions. Our results are for the single-particle spectral weight $A(k; \cdot)$ at the wave-vector $k = (0; \cdot)$ but qualitatively similar data is obtained at $k = (\pi/2; \cdot)$. At the latter point the pseudogap is smaller however, as expected [6]. The results are enclosed by the statistical uncertainty, by the systematic error introduced through imaginary-time discretization, Δt , and by the finite size, L , of the system. The two calculations with $\Delta t = 1/10$ in Fig.2a show that increasing the number of QMC sweeps (smaller Δt , denoted in Fig.2) leads to a more pronounced pseudogap. The same figure also shows calculations with the same Δt but different values of L (systematic error is of order $(L)^2$). For $L = 10$, the systematic decrease in pseudogap depth with decreasing L becomes less than the accuracy achievable by the maximum entropy inversion. If the pseudogap persists when $L = 1$ at fixed Δt and $\Delta t = 1/10$ it should be even more so with a larger number of QMC sweeps (smaller Δt). The size analysis needs to be done however since increasing the system size L at fixed Δt leads to a smaller pseudogap, as shown on the top left panel of Fig.3a.

It is customary to analytically continue imaginary time QMC using the Maximum Entropy algorithm [10]. To provide a faithful comparison with the many-body approaches, we use the imaginary-time formalism for these methods and analytically continue them for the same number of imaginary-time points, using precisely the same Maximum entropy approach as for QMC. While the round off errors in the many-body approaches are very small, it is preferable to artificially set them equal to those in the corresponding QMC simulations to have

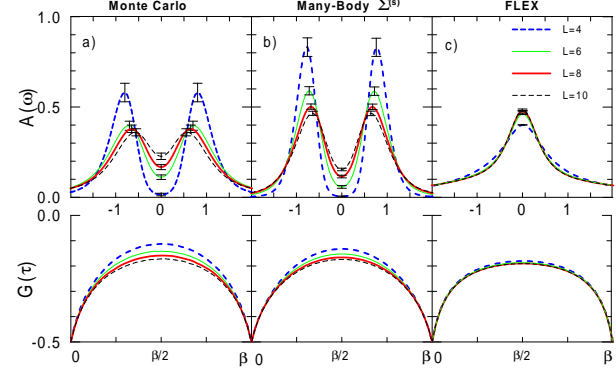


FIG. 3. Size dependent results for various types of calculations for $U = 4$, $\beta = 5$, $n = 1$, $k = (0; \cdot)$, $L = 4; 6; 8; 10$ and average relative errors $\sigma = 3.4\%$ on $G(\cdot)$. Upper panels show $A(k; \cdot)$ extracted from Maximum Entropy on $G(\cdot)$ shown on the corresponding lower panels. Each $G(\cdot)$ has 50 points. (a) QMC. (b) Many-body using Eq.(3). (c) FLEX.

the same degree of smoothing. Many-body results from the symmetric self-energy formula $\Sigma^{(s)}$; Eq.(3) for an infinite system are shown in Fig.2b. The thin solid line is a direct real-frequency calculation in the infinite-size limit. Maximum Entropy inversions of the $L = 1$ value of the many-body $G(\cdot)$ shown on the same figure illustrate that with increasing accuracy the real-frequency result is more closely approximated. This confirms that Maximum Entropy simply smooths the results when artificially large errors are introduced in the analytical results. [12] For this parameter range, the effects are appreciable but do not change qualitatively the results. Even the widths of the peaks are not too badly reproduced by Maximum Entropy. The error bars are obtained from the Maximum Entropy Bayesian probability for different regularization parameters: [10] They are clearly a lower bound.

In Fig.3, we show the spectra obtained for three techniques for system sizes $L = 4; 6; 8$ and 10. The left-hand panel is the QMC data, the middle panel is obtained from Eq.(3) while the last panel is for FLEX. The latter results for much larger lattices are not much different from those for the 8 × 8 system. The FLEX method displays a maximum at $\tau = 0$ contrary to the Monte Carlo results. By contrast, as can be seen by comparing the middle and left panels, the agreement between Eq.(3) and QMC is very good, except for the height of the peaks. The finite-size dependence of the pseudogap for both QMC and Eq.(3) is similar: as the size increases, the depth of the pseudogap decreases. Some of the finite-size effects are present in the vertices U_{sp} and U_{ch} . Fig.4a compares three results for the $L = 6$ system: QMC (thick solid line), and the many-body approach of Ref. [7] using either the symmetric $\Sigma^{(s)}$ (Eq.(3), dotted line) or the longitudinal $\Sigma^{(l)}$ (Eq.(2), thin solid line) self-energy formulas. In imaginary time, the agreement between QMC and

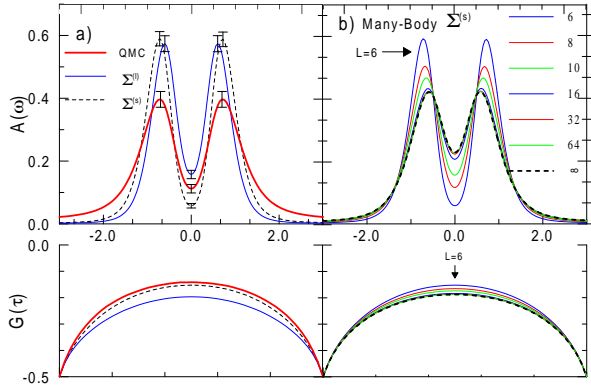


FIG. 4. $U = 4$, $\gamma = 5$, $n = 1$, $\mathbf{k} = (0; 0)$, and $\omega = 3.2\%$ in Maximum Entropy. (a) For $L = 6$, thick solid line for QMC, and Many Body using two different self-energy formulas: dashed line for symmetric Eq.(3), and thin solid line for longitudinal Eq.(2). (b) Size dependent results obtained from symmetric version Eq.(3) for $L = 6; 8; 10; 16; 32; 64$ and infinite size (dashed line). The size dependence is monotonic.

$\Sigma^{(s)}$ is striking. The position of the peaks in QMC also agrees better with the symmetric version $\Sigma^{(s)}$, Eq.(3).

For the lattice sizes where the Monte Carlo data are qualitatively similar to those of Ref. [8], and hence uncontroversial, Fig. 3 has shown that there is a many-body approach that gives good agreement with the simulations. Although this many-body approach is not rigorous, especially deep in the pseudogap regime where it is mostly an extrapolation method [7], these tests suggest that it can give an understanding of finite-size effects in QMC data. There are two intrinsic lengths that are relevant, namely the antiferromagnetic correlation length, and the single-particle thermal Bogoilev wavelength defined by $v_F = T$: If we had $\tau_h > L$, one would be effectively probing the finite-size zero-temperature quantum regime. When the condition $L > \tau_h$ is satisfied one has access to the finite temperature effects we are looking for. Once agreement on the pseudogap in QMC and the analytical approach has been established up to the regime $\tau_h < L < \tau_h$, the analytical approach [7] can be used to reach larger lattice sizes (such that $\tau_h < \tau_h < L$) with relatively modest computer effort. At the $(0; 0)$ point, τ_h essentially vanishes since we are at the van Hove singularity, hence the condition $\tau_h < L$ is satisfied. In Fig. 4b we show the spectra obtained by Eq.(3) for $L = 6$ to 64 and then for $L = 1$ (obtained from numerical integration). We see that the size dependence of the pseudogap becomes negligible around $L = 32$ and that the pseudogap is quite sizable even though it is smaller than that in the largest size available in QMC calculations ($L = 10$): The size dependence of the pseudogap is qualitatively similar when the longitudinal form of the self-energy is used. We thus conclude that the pseudogap exists in the thermodynamic limit, contrary to the

conclusion of Ref. [8]. The physical origin of the pseudogap in the 2D Hubbard model as well as the reason for the failure of FLEX-type approaches have been discussed at great length previously [7]: The precursors of antiferromagnetism in $A(\mathbf{k}_F; \omega)$ are preformed Bogoliubov quasiparticles that appear as a consequence of the influence of critical spin fluctuations in two dimensions. Strong-coupling particle-hole pairs are not necessary to obtain a pseudogap.

In conclusion, we have shown, through comparisons with QMC simulations, that a method that takes both Green functions and vertex corrections into account at a consistent level of approximation is more accurate in describing the low-temperature behavior of the 2D half-filled Hubbard model than self-consistent Eliashberg-type methods such as FLEX that include renormalized Green functions but no vertex corrections in a context where there is no Migdal theorem to justify this neglect of vertex corrections. The latter methods give results that are qualitatively wrong for the pseudogap.

S.M. benefited from a useful correspondence with S.R. White and from discussions with J. Deisz. Contributions to the code from H. Touchette are gratefully acknowledged. Monte Carlo simulations were performed in part on an IBM-SP2 at the Centre d'Applications du Calcul Parallèle de l'Université de Sherbrooke. This work was supported by a grant from the Natural Sciences and Engineering Research Council (NSERC) of Canada and the Fonds pour la formation de Chercheurs et l'Aide à la Recherche (FCAR) of the Québec government.

- [1] J. E. Hirsh, Phys. Rev. B 31, 4403 (1985).
- [2] S. R. White, et al., Phys. Rev. B 40, 506 (1989).
- [3] N. E. Bickers and D. J. Scalapino, Annals of Physics, 193, 206 (1989); N. E. Bickers, D. J. Scalapino and S. R. White, Phys. Rev. Lett. 62, 961 (1989).
- [4] J. J. Deisz, D. W. Hess and J. W. Serene, Phys. Rev. Lett. 76, 1312 (1996).
- [5] Y. M. Vilk, Liang Chen, A.-M. S. Tremblay, Phys. Rev. B 49, 13267 (1994).
- [6] Y. M. Vilk and A.-M. S. Tremblay, Europhys. Lett. 33, 159 (1996).
- [7] Y. M. Vilk and A.-M. S. Tremblay, J. Phys. France 7, 1309 (1997).
- [8] M. Vekic and S. R. White, Phys. Rev. B 47, 1160 (1993).
- [9] C. E. Cress et al., Phys. Rev. Lett. 75, 517 (1995).
- [10] M. Jarrell and J. E. Gubernatis, Phys. Rep. 269, 133 (1996). R. K. Bryan, Eur. Biophys. J. 18, 165 (1990).
- [11] N. Bulut et al., Phys. Rev. B 47, 2742 (1993); N. F. Berk and J. R. Schrieffer, Phys. Rev. Lett. 17, 433 (1966).
- [12] For small lattices, the many-body approach of Ref. [7] predicts many sharp peaks, as expected from the discreteness of the energy levels.